Solar/Wind Hybrid Energy Harvesting for Supercapacitor-based Embedded Systems

Mohamadhadi Habibzadeh*, Moeen Hassanalieragh†, Tolga Soyata*, Gaurav Sharma†
*Department of Electrical and Computer Engineering, SUNY Albany, Albany, NY 12203
†Department of Electrical and Computer Engineering, University of Rochester, Rochester, NY 14627
{hhabibzadeh, tsoyata}@albany.edu*, {m.hassanalieragh, gaurav.sharma}@rochester.edu†

***Abstract*—For autonomous medium power (1–10 W) field systems deployed in off-grid applications without established power infrastructure, two system design criteria are crucially important: i) continuous availability of power, ii) robust and low-maintenance operation. In this paper, we provide circuit and system designs for energy harvesters that address both issues by utilizing supercapacitors as their energy buffer and hybrid solar and wind power sources for their power supply. By utilizing the complimentary nature of solar and wind power sources, the necessity for large supercapacitor buffers is eliminated. Although a rich body of solar-only designs exist in the literature, in our knowledge, this is the first paper that demonstrates a hybrid harvester design for the medium power range. We experimentally demonstrate the functionality of our harvester designs.**

***Index Terms*—Hybrid energy harvesting; wind power harvesting; embedded systems; solar power harvesting.**

I. Introduction

A rich body of medium-power (1–10 W) harvester designs exist in the literature for *solar-only* power input, which is the most common power supply for embedded field systems [1]–[3]; to ensure robust and low-maintenance operation, supercapacitors are commonly used in these systems as the sole energy buffer [4]. When solar is the sole power source, a large supercapacitor block must be used to compensate for the unavailability of solar power at night (or cloudy days), which drastically increases system cost and physical footprint. Hybrid power sources (solar and wind) provide a complimentary availability because the lack of power during cloudy days are partly compensated by the availability of wind [5].

Existing designs focus on μW and mW range harvesters [6], [7], in our knowledge, this is the first paper that demonstrates a working prototype of a medium power (1–10 W), supercapacitor-based hybrid harvesting system that can be modularly expanded to incorporate multiple solar and wind power sources. Our expandable design uses a single solar-only harvester and provides a platform expandable to multiple solar and multiple wind power sources buffering all harvested energy into a single supercapacitor block. We investigate the necessary peripheral circuit components, as well as the necessary firmware, to permit this modular design. We demonstrate the functionality of our designs experimentally through an actual supercapacitor-based harvester that harvests a 50 W-rated wind turbine and a 30 W-rated rated solar panel.

The rest of this paper is organized as follows: In Section II, we describe the architecture of a generalized harvester. In Section III, we discuss the necessary hardware/firmware changes to turn a commonly-available solar-only harvester into a wind-only harvester. Based on this foundation, we expand our design to provide hybrid harvester designs in Section IV and investigate their expandability. We provide experimental evaluation results and concluding remarks in Section V.

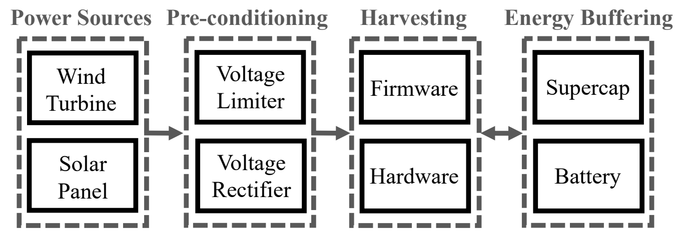

Figure 1: Generalized system architecture of an energy harvester capable of harvesting hybrid power sources.

II. Harvesting Systems

Figure 1 depicts a generalized system architecture of a harvester that is capable of harvesting multiple power sources. This architecture consists of four components:

A. Power Sources

This component includes the transducers that generate electric power by harvesting ambient power sources. Although different ambient power sources such as thermal [8], vibration [9], and RF [7] can be utilized for μW and mW power sources, the only two options that are suitable for supplying medium power ranges (1–10 W) are solar panels and wind turbines. Our particular focus in this paper is field applications that require autonomous operation, low maintenance, and a significant amount of computing power; for example, in environmental monitoring, recognition of different bird species requires intensive image processing [10], which can only be achieved using a computational device that incorporates a multi-core ARM processor (e.g., an Android tablet). Such devices have been reported to consume 1–5 W just for computations and more when WiFi or USB are turned-on, hence our definition of "medium-power range of 1–10 W."

B. Pre-conditioning

Because the harvester requires a DC voltage, AC voltage sources (such as wind turbines) require a rectifier before they can be used by the harvester. Furthermore, voltage levels at the

Power Sources component are highly dependent on ambient conditions; in cases where this voltage level exceeds the allowed maximum of the *Harvesting* component specifications, a "voltage limiter" is required before the power source is applied to the harvester. We term the combination of these two *auxiliary* circuits the *Pre-conditioning* component.

C. Harvesting

Hardware in this component includes a SEPIC DC-DC converter and its microcontroller firmware executes a Maximum Power Point Tracking (MPPT) algorithm [2] to harvest the maximum amount of energy from the power source.

D. Energy Storage

Many harvesting systems incorporate an *Energy Buffering* component to buffer the surplus portion of the harvested energy, which can be used later to compensate for lack of power when the ambient power source is temporarily unavailable (e.g., during nights for solar energy harvesters). *Energy Storage* components are typically implemented using batteries, supercapacitors, or a combination of both.

III. Wind Energy Harvesting

Our goal in this paper is to conceptualize a modularized system design from an existing solar-only harvester that incorporates a microcontroller; such a design allows easy expansion to wind power sources by implementing a different MPPT algorithm in its firmware and adding a rectifier and a voltage limiter if the voltage output of the wind turbine exceeds the specified maximum of the solar-only harvester. Figure 2 (top) depicts an open-source solar-only design [11] that we utilize in our experiments, which implements the fractional-V_{OC} MPPT algorithm for solar harvesting in its firmware. Figure 2 (bottom) depicts how a wind harvester can be implemented from this solar-only harvester by adding a rectifier and a voltage limiter and by implementing a wind MPPT algorithm. In this section, we describe each component.

A. Wind Energy Harvester Components

Power Source: For the wind turbine, we use a conventional permanent-magnet horizontal axis wind turbine.

Pre-conditioning: The rectifier composed of six Schottky diodes and a capacitor converts the three-phase AC wind turbine output into DC. The wind turbine we utilize can generate up to 50 V under high-speed winds. Our voltage limiter in Figure 2 (bottom) turns on the MOSFET and shunts the excess wind turbine current when the wind turbine voltage exceeds ≈25 VDC (which is the limit for the solar-only harvester) using the 24 V Zener diode (1N4749). This causes the MOSFET to dissipate the excess power and requires a heat sink to dissipate the generated heat; in our practical implementation, we used six parallel MOSFETs to substantially reduce the dissipation on each transistor.

Harvester: The solar-only harvester employs a fractional open circuit voltage MPPT algorithm to calculate the MPP voltage. It then maintains this voltage by applying the proper duty cycle (D) to the switching MOSFET of its embedded DC-DC SEPIC controller, which, as formulated in [12], serves as a variable load between the buffer and the source. Fractional open voltage MPPT algorithm is not suitable for wind power sources. We, therefore, developed a new firmware that uses the Hill Climbing (HC) [13] MPPT algorithm instead. Details of our hardware/software implementations along with their open source designs are provided in [14].

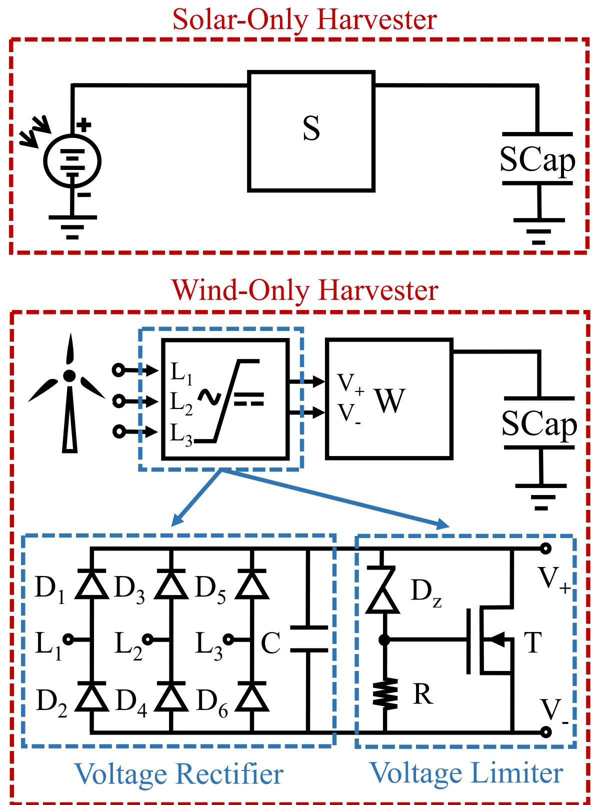

Figure 2: Design of a wind harvester from a solar-only harvester by adding a rectifier and a voltage limiter.

Energy Buffer: Both the solar-only and wind-only harvesters use a block of eight 3000 F supercapacitors for energy buffering, equating to 23.6 Wh energy storage capacity.

B. Required Input Buffer Capacitor

Figure 3a depicts the *input buffer capacitor* required to keep the wind V_{MPP} voltage stable while the HC algorithm is adjusting this voltage in the *Harvester* component. Adjusting V_{MPP} implicitly controls the current drawn from the wind turbine (I_{Wind}). The current that is drawn by the SEPIC harvester (I_{SEPIC}) is a function of whether the HC algorithm is attempting to increase or decrease the V_{MPP} based on instantaneous wind conditions. This brings about two scenarios:

$$\begin{cases} I_{SEPIC} > I_{Wind} & C_{in} \text{ is discharging} \\ I_{SEPIC} = I_{Wind} & C_{in} \text{ is by-passed} \\ I_{SEPIC} < I_{Wind} & C_{in} \text{ is charging} \end{cases} \tag{1}$$

Note that the only control the HC algorithm has is the I_{SEPIC} through adjusting the duty cycle (D) of the SEPIC DC-DC converter. At any instant, the voltage of the wind turbine

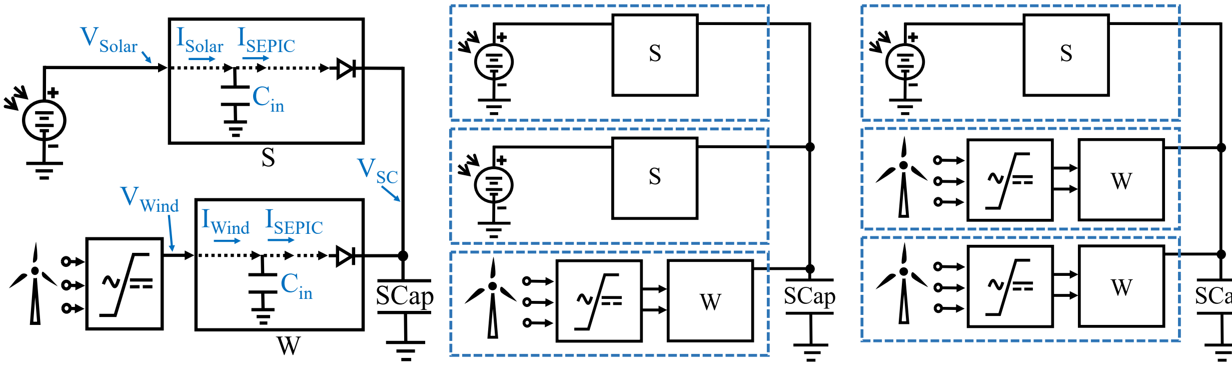

(a) *SW* (b) *SSW* (c) *SWW*

Figure 3: Three example configurations of our proposed hybrid harvesting. The modularity of our architecture allows us to implement a variety of hybrid energy harvesters by incorporating additional solar- and wind-only harvesters.

(V_{Wind}) can be higher or lower than the desired V_{MPP} value for harvesting the maximum power.
The harvester adjusts D to get $V_{Wind}{=}V_{MPP}$ as follows:

$$\begin{cases} V_{Wind} > V_{MPP} & \text{increase } D \quad I_{SEPIC} \Uparrow \\ V_{Wind} = V_{MPP} & \text{keep } D \\ V_{Wind} < V_{MPP} & \text{decrease } D \quad I_{SEPIC} \Downarrow \end{cases} \tag{2}$$

Maximum C_{in} value can be computed from these conditions. We first analyze the scenario $V_{wind} > V_{MPP}$ and consequently $I_{wind} > I_{MPP}$; SEPIC reduces its voltage $V_{wind} \rightarrow V_{MPP}$ by increasing its D, which discharges C_{in}. This requires three distinct steps, tabulated in Table I. Each step transfers a certain amount of energy from C_{in} into the supercapacitor block (i.e., *harvests*), quantified as:

$$\begin{aligned} E_1 &= \frac{1}{2} \cdot (I_{wind} + I_{SEPIC}^{max}) \cdot V_{wind} \cdot \Delta t_1, \\ E_2 &= I_{SEPIC}^{max} \cdot \frac{1}{2} \cdot (V_{wind} + V_{MPP}) \cdot \Delta t_2, \\ E_3 &= \frac{1}{2} \cdot (I_{SEPIC}^{max} + I_{MPP}) \cdot V_{MPP} \cdot \Delta t_3. \end{aligned} \tag{3}$$

Their sum equals the energy wind turbine supplied during these three steps (E_{wind}) and the energy C_{in} lost ($E_{C_{in}}$):

$$E_1 + E_2 + E_3 = E_{wind} + E_{C_{in}}, \tag{4}$$

$$\begin{aligned} E_{C_{in}} &= \frac{1}{2} \cdot C({V_{wind}}^2 - {V_{MPP}}^2), \\ E_{wind} &= \frac{1}{4} \cdot (I_{MPP} + I_{wind})(V_{MPP} + V_{wind}) \cdot \Delta t. \end{aligned} \tag{5}$$

where $\Delta t = \Delta t_1 + \Delta t_2 + \Delta t_3$. Using a piecewise linear approximation for these three phases, we can calculate:

$$\begin{aligned} C_{in}^{max1} &= \frac{2}{V_{wind}^2 - V_{MPP}^2} \cdot \left(\frac{E_1 + E_2 + E_3}{E_{wind}} \right), \\ C_{in}^{max2} &= \frac{2}{V_{MPP}^2 - V_{wind}^2} \cdot \left(\frac{E_{wind}}{E_1 + E_2 + E_3} \right), \\ C_{in}^{max} &= min(C_{in}^{max1}, C_{in}^{max2}). \end{aligned} \tag{6}$$

where C_{in}^{max2} is the opposite condition when C_{in} is *charging*.

The **minimum C_{in} value** (C_{in}^{min}) is determined by the maximum tolerable ripple in V_{MPP} (ΔV_{MPP}) by using a linear approximation in the current and voltage ripples:

$$C_{in}^{min} = \frac{1}{2} \cdot \frac{I_{wind}^{max}}{\Delta V_{MPP}} \Delta t_1 \tag{7}$$

Practical Example: Using practical values $I_{wind} = 3\,\text{A}$, $I_{MPP}{=}2\,\text{A}$, $I_{SEPIC}^{max}{=}4\,\text{A}$, $V_{wind}{=}20\,\text{V}$, and $V_{MPP} = 15\,\text{V}$, and $\Delta t_1 = 1\,\text{ms}$, $\Delta t_2 = 9\,\text{ms}$, and $\Delta t_3 = 1\,\text{ms}$, which are realistic values determined by wind turbine characteristics and computational power of the microcontroller, Eq. 6 yields $C_{in}^{max1} \approx 18000\,\mu\text{F}$ and $C_{in}^{max2} = 129000\,\mu\text{F}$, therefore $C_{in}^{max} \approx 18000\,\mu\text{F}$. Furthermore, if we assume $I_{wind}^{max} = 3\,\text{A}$ and $\Delta V_{MPP}{=}1\,\text{V}$, Eq. 7 yields $C_{in}^{min}{=}1500\,\mu\text{F}$. Therefore, the optimal C_{in} is $1500\,\mu\text{F} < C_{in} < 18000\,\mu\text{F}$. In our actual design, we used $C_{in} = 4700\,\mu\text{F}$.

Table I: Three phases of SEPIC current and voltage transitions

Δt	D	$V_{C_{in}} = V_{SEPIC}$	I_{SEPIC}	$I_{C_{in}}$
Δt_1	$\Uparrow$	$\Leftrightarrow V_{wind}$	$\Uparrow I_{wind} \rightarrow I_{SEPIC}^{max}$	Disch.
Δt_2	$\Leftrightarrow$	$\Uparrow V_{wind} \rightarrow V_{MPP}$	$\Leftrightarrow I_{SEPIC}^{max}$	Disch.
Δt_3	$\Downarrow$	$\Leftrightarrow V_{MPP}$	$\Downarrow I_{SEPIC}^{max} \rightarrow I_{MPP}$	Disch.

IV. Hybrid Solar/Wind Energy Harvesting

In Section III, we used a solar only harvester to design a wind-only harvester. We will use the notations S and W to denote these two harvesters, respectively. We will now expand on this foundation to introduce our *hybrid* harvester designs, which are capable of harvesting more than one power source.

A. Hybrid Solar/Wind Energy Harvester

Figure 3 depicts the high-level implementation of our first hybrid solar/wind harvester, which we refer to as the SW configuration. It consists of a single solar-only (S) and a single wind-only (W) harvester operating independently. The output of each of these single-source harvesters is connected to the same supercapacitor block. The Schottky diodes within the SEPIC converters (Fig. 3a) prevent charge from erroneously flowing from one harvester into the other [11].

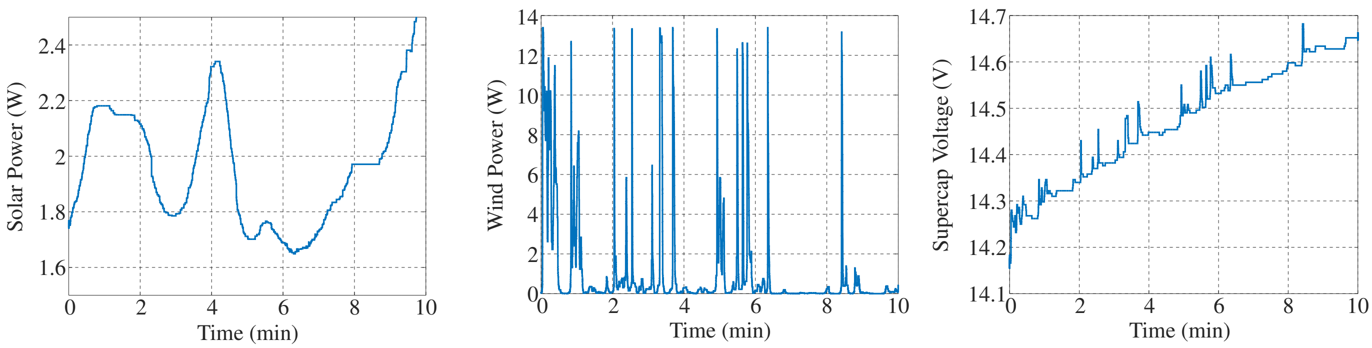

Figure 4: Experimental results for the SW harvester. Far left plot shows the output power of solar panel, while the middle plot shows the output power of the wind turbine. The voltage of the supercapacitor energy storage block is depicted in the far right sub-figure. During this period, $\widehat{P}_{solar} \approx 2\,\text{W}$ and $\widehat{P}_{wind} \approx 1.7\,\text{W}$ and the average cumulative incoming poweris $\widehat{P} \approx 3.7\,\text{W}$.

B. Modular Expansion of Hybrid Energy Harvesters

The modularity of this harvester design enables us to readily modify the SW configuration to incorporate other types of power sources. For example, replacing the wind-only harvester in Fig. 3 with a solar-only one converts the system into an SS configuration, which can also be considered to be a "hybrid" harvester if the solar panels are placed at different locations/orientations; different angles/orientations allow the solar panels to have complementary power availability patterns, as the generated power of each panel changes based on its relative orientation towards the sun. Similarly, WW harvesting system can be implemented by utilizing two wind-only harvesters. Suitable applications for such systems include mountainous areas, where wind availability patterns can change abruptly based on location. Moreover, systems that include more than two power sources such as WWW, SSW, SWW, and SSS can be implemented as shown in Fig. 3. In-depth analysis of these configurations is available in [14].

V. Evaluation and Conclusions

Figure 4 shows the performance of our SW hybrid harvester, which utilizes an S harvester with a 30 W solar panel and our firmware-modified version W harvester with a Higoo™ 50 W residential wind turbine as our wind power source. Our energy buffer is 8 serially-connected Maxwell 3000 F supercapacitors. Starting from the left, the first sub-figure depicts the instantaneous harvested power from the solar panel, the second sub-figure depicts the harvested power from the wind turbine, and the last figure shows the instantenous voltage of the supercapacitor block. As observed in Fig. 4, the supercapacitor block starting voltage is $V_{start} = 14.24\,\text{V}$, which rises to $V_{end} = 14.65\,\text{V}$ after an observation period of 10 minutes. The total harvested energy is $E_{end} - E_{start} = 0.5 \times \frac{3000}{8} \times (14.65^2 - 14.24^2) = 2221$ Joules. We can infer that the average incoming power in 10 minutes is $\widehat{P} = \widehat{P}_{solar} + \widehat{P}_{wind} = 2221/600 \approx 3.7\,\text{W}$. Averaging the data depicted in Fig. 4, we calculate $\widehat{P}_{solar} \approx 2.0\,\text{W}$ and $\widehat{P}_{wind} \approx 1.7\,\text{W}$ during the 10 minute harvesting period; the experimental result of 3.7 W for the average of the two hybrid sources is consistent with their sum, thereby confirming the functionality of our SW harvester.

References

[1] F. I. Simjee and P. H. Chou, "Efficient charging of supercapacitors for extended lifetime of wireless sensor nodes," *IEEE Transactions on Power Electronics*, vol. 23, no. 3, pp. 1526–1536, May 2008.

[2] D. Brunelli, C. Moser, L. Thiele, and L. Benini, "Design of a solar-harvesting circuit for batteryless embedded systems," *IEEE TCASI: Regular Papers*, vol. 56, no. 11, pp. 2519–2528, Nov 2009.

[3] H. Habibzadeh, Z. Qin, T. Soyata, and B. Kantarci, "Large Scale Distributed Dedicated- and Non-Dedicated Smart City Sensing Systems," *IEEE Sensors Journal*, 2017, Accepted for Publication.

[4] M. Hassanalieragh, T. Soyata, A. Nadeau, and G. Sharma, "Solar-Supercapacitor Harvesting System Design for Energy-Aware Applications," in *Proceedings of the 27th IEEE International System-on-Chip Conference (IEEE SOCC)*, Las Vegas, NV, Sep 2014, pp. 280–285.

[5] S. Rao and N. B. Mehta, "Hybrid energy harvesting wireless systems: Performance evaluation and benchmarking," in *2013 IEEE WCN Conference)*, April 2013, pp. 4244–4249.

[6] N. Kong and D. S. Ha, "Low-Power Design of a Self-powered Piezoelectric Energy Harvesting System With Maximum Power Point Tracking," *IEEE TPEL*, vol. 27, no. 5, pp. 2298–2308, May 2012.

[7] T. Soyata, L. Copeland, and W. Heinzelman, "RF Energy Harvesting for Embedded Systems: A Survey of Tradeoffs and Methodology," *IEEE Circuits and Systems Magazine*, vol. 16, no. 1, pp. 22–57, Feb 2016.

[8] M. Ashraf and N. Masoumi, "A thermal energy harvesting power supply with an internal startup circuit for pacemakers," *IEEE Transactions on VLSI Systems*, vol. 24, no. 1, pp. 26–37, Jan 2016.

[9] Y. Zhu, Y. Zheng, Y. Gao, D. I. Made, C. Sun, M. Je, and A. Y. Gu, "An energy autonomous 400 mhz active wireless saw temperature sensor powered by vibration energy harvesting," *IEEE Transactions on Circuits and Systems I: Regular Papers*, vol. 62, no. 4, pp. 976–985, April 2015.

[10] Allan F O'Connell, James D Nichols, and K Ullas Karanth, *Camera traps in animal ecology: methods and analyses*, Springer Science & Business Media, 2010.

[11] M. Hassanalieragh, T. Soyata, A. Nadeau, and G. Sharma, "UR-SolarCap: An Open Source Intelligent Auto-Wakeup Solar Energy Harvesting System for Supercapacitor Based Energy Buffering," *IEEE Access*, vol. 4, pp. 542–557, Mar 2016.

[12] Kenji Amei, Yukichi Takayasu, Takahisa Ohji, and Masaaki Sakui, "A maximum power control of wind generator system using a permanent magnet synchronous generator and a boost chopper circuit," in *Power Conversion Conference, 2002. PCC-Osaka 2002. Proceedings of the*. IEEE, 2002, vol. 3, pp. 1447–1452.

[13] E. Koutroulis, K. Kalaitzakis, and N. C. Voulgaris, "Development of a Microcontroller-based, Photovoltaic Maximum Power Point Tracking Control System," *IEEE TPEL*, vol. 16, no. 1, pp. 46–54, Jan 2001.

[14] M. Habibzadeh, M. Hassanalieragh, A. Ishikawa, T. Soyata, and G. Sharma, "Hybrid Solar-Wind Energy Harvesting for Embedded Applications: Supercapacitor-based System Architectures and Design Tradeoffs," *IEEE Circuits and Systems Magazine*, 2018, Accepted for Publication.